PHYSICAL REVIEW B VOLUME 25, NUMBER 12 15 JUNE 1982

Final-state rule for Auger line shapes

David E. Ramaker
Department of Chemistry, George Washington University, Washington, D.C. 20052
(Received 30 December 1981)

A final-state (FS) rule is proposed and tested for the Auger process. This rule is similar to the FS rule and the orthogonalized-final-state (OFS) rule already in existence for x-ray emission and absorption. The FS rule can be stated as follows: In the absence of significant configuration mixing, the initial state determines separately the *ss*, *sp*, and *pp* Auger intensities; the shape of each contribution is determined by the final density of states (DOS). Several Auger line shapes are examined in the context of this FS rule. In the molecules NO_3^-, O_2, and C_2H_6, core-hole-state calculations indicate screening significantly alters the ground-state molecular orbital *p* populations. The experimental Auger peak intensities, however, reflect *p* populations similar to the ground state. In the metals Be and Cu, the *s* electrons dominate the core-hole screening charge. This significantly increases the *ss* and *sp* contributions relative to the *pp*, which is indicated by the experimental Auger line shape. The individual *ss*, *sp*, and *pp* line shapes, however, reflect the final DOS. The Auger line shapes of the C_8Cs and C_6Li intercalated graphite systems reflect a valence band appropriate to the final state; however, they exhibit a much larger intercalant peak intensity compared to photoemission data. This is discussed in light of the OFS rule.

I. INTRODUCTION

From a theoretical viewpoint, the Auger process is a complicated dynamical process exhibiting several interesting phenomena. These include (i) atomic relaxation and electron screening in response to creation of the initial core hole, (ii) possible localization of the Auger final-state holes as a result of election correlation, and (iii) a possible "Coulomb explosion" or dissociation of the molecule or local cluster as a result of the localized holes. In an effort to develop a semiempirical approach to near quantitive Auger-line-shape interpretations, we have previously reported our studies of the latter two phenomena.[1-3] In this work we examine the effects of electron screening on the Auger line shape and develop a simple approach for including these effects in a theoretical determination of the line shape.

The response of the valence electrons to the creation of a core hole takes several forms. In simple atoms the orbitals usually contract around a core hole, this is normally referred to as atomic relaxation. In molecules and solids the bonds also polarize, i.e., electron density in a bonding orbital flows toward the core hole, in an antibonding orbital it flows away from the hole. In the event the bonding and antibonding orbitals (or band in the case of the solid) are not completely filled, a net "charge transfer" to the atom with the core hole results. This local screening charge is seen to be predominantly *s*-like in the *sp*-band metals [e.g., Na, Mg, and Al (Ref. 4), Be (Ref. 5), and Cu (Ref. 6)]. In some metals this screening charge may be sufficiently polarized as to produce a localized or excitonic state.[7,8] In insulators and semiconductors, the creation of an electron-hole pair may introduce a defect or excitonic state in the band gap.[9] The screening may also involve a more nonlocal accumulation of charge around the core hole (plasmon), or in metals create electron-hole pairs giving rise to an edge singularity.[10]

A great deal of attention has been given to the effect of screening in the x-ray emission and absorption of simple metals particularly near the edge or threshold.[11] The asymptotic version of the many-body theory of Mahan-Nozières-De Dominicis (MND) predicts the well-known edge singularities which occupy the narrow energy range < 1.0 eV near threshold. Further removed from the threshold an exact MND calculation is required, but this is much more difficult. Thus it is often asserted that a one-electron theory is adequate in this region. By performing numerical studies of the exact MND theory, von Barth and Grossmann[12] and also Mahan[13] have shown that

indeed a one-electron theory is adequate away from threshold provided the one-particle wave functions are calculated using the potential of the final state (i.e., in the presence of a core hole for absorption, without a core hole for emission). Basic sum rules as shown by Grebennikov *et al.*[14] show, however, that the total intensity of the emission or absorption spectrum must be equal to the intensity obtained when using the one-particle wave functions appropriate for the initial state. These results have been formulated into a "final-state (FS) rule" which states that the area under an emission or absorption spectrum is given by the initial state; its shape by the final state.[13]

Recently Davis and Feldkamp[15] presented a simple derivation indicating why the FS rule is reasonable, and further showed that it can be improved by orthogonalization of the final-state hole orbitals to the existing initial-state hole orbitals. This shall be referred to as the orthogonalized-final-state (OFS) rule. From numerical studies it has been shown to improve on the FS rule primarily near the threshold where it accounts for some of the edge singularity effects.

In this work we will utilize the methods of Davis and Feldkamp[15] to show the existence of FS and OFS rules also for the two-electron Auger process. The use of the rules in the context of our previously derived methods for a determination of the Auger and shake-Auger line shapes (the latter yet another result of core-hole screening) will be indicated. Finally, the validity of the FS and OFS rules for the Auger process will be shown by examining Auger line-shape interpretations previously reported for the molecules O_2 and C_6H_6, the metals Be and Cu, and the nonmetals $LiNO_3$, Si, and C_6Li (intercalated graphite).

II. THEORY

A. The FS and OFS rules for the Auger process

The Auger transition rate $W^A(E)$ is normally obtained from the first-order perturbation-theory result of Wentzel,[16]

$$W^A(E)=\frac{2\pi}{\hbar}\sum_m |\langle \psi^f_m | V | \psi^i \rangle|^2 \delta(E+E^f_m-E^i) , \tag{1}$$

where the superscripts f and i refer to final and initial states, respectively, and $V=H-H^0$, in the one-electron approximation, is normally set equal to $\sum_{i<j} r_{ij}^{-1}$. As such, Eq. (1) is valid only when ψ^f_m and ψ^i are eigenfunctions of the same Hamiltonian H, which of course is not the case in a valence orbital picture where ψ^i and ψ^f are evaluated under different potentials (i.e., with and without a core hole). In this instance it is more appropriate to use $V=H-E$ which includes any residual interaction between the initial and final states.[17,18]

Equation (1) is also based on the two-step model in which the Auger decay is assumed to be independent of the creation of the initial core hole. It assumes that by the time the Auger event occurs the relaxation and screening of the core hole is complete, i.e., it assumes the screening time is short compared to the core-hole lifetime. The screening time τ depends on the screening mechanism of the system involved.[19–21] τ is of the order $\hbar/E_x$, where E_x is the ion excitation energy of the process involved.[22] Typical times for the local excitonic process can be related to the conduction bandwidth ($\sim 5-10$ eV), the collective process to the plasmon frequency ($1-10$ eV), and the slower pair shakeup response to the line asymmetry ($\sim 0-1.0$ eV).[22] In insulators, the screening may result from the polarization of the bonding and antibonding orbitals and thus may be related to the larger covalent interaction (i.e., to the band gap) or again to the larger plasmon frequency ($\sim 15-30$ eV). Electron-hole pair shakeup is not important in insulators. This suggests the relaxation time may be shorter in insulators; however, since the polarization energy resulting from the core hole may be less than $15-30$ eV, the dominant screening may occur through other mechanisms (e.g., involving virtual excitations) giving a slower screening response. In any event the extent of the screening response is smaller in insulators. Typical shallow core-hole widths are of the order $\sim 0.01-1.0$ eV with only the deeper core holes having widths > 1.0 eV.[23] Generally it seems that the two-step model is valid, particularly for *CVV* Auger line shapes as treated in this work. A dynamical theory of the Auger process which allows for incomplete screening has been recently reported by Gunnarsson and Schonhammer[24] and Ohno and Wendin.[25] These results show that incomplete screening can alter both the energy and line shape of the Auger spectra.

For the Auger process let us write the initial and final states in terms of the hole orbitals (following Ref. 15),

$$\psi_l^i = |\,\phi_c\bar{\epsilon}_l\phi'_K\bar{\phi}'_K\cdots\phi'_N\bar{\phi}'_N\,|\ , \tag{2}$$

$$\psi_{ij}^f = |\,\phi_i\bar{\phi}_j\phi_K\bar{\phi}_K\cdots\phi_N\bar{\phi}_N\,|\ , \tag{3}$$

where we assume for simplicity single-determinant wave functions. Here $K,K+1,\ldots,N$ label the hole orbitals in a single-band model; the initial and final orbitals evaluated in the presence or absence of a core hole are indicated by the "primed" and "unprimed" orbitals, respectively. $\bar{\phi}$ indicates orbitals with spin down, ϕ those with spin up. The holes ϕ_i and $\bar{\phi}_j$ arise as a result of the Auger process, the Auger electron escaping with energy ϵ in the continuum orbital $\bar{\epsilon}_l$, the other electron droping into the core orbital ϕ_c.

The transition matrix element can be reduced to the two-electron integral expression,

$$\left\langle \psi_l^i \,|\, V \,|\, \psi_{ij}^f \right\rangle = \int\int d\tau_1 d\tau_2 \begin{vmatrix} \phi_c\phi_i & \phi_c\phi_K & \cdots & \phi_c\phi_N \\ S_{iK} & S_{KK} & \cdots & S_{NK} \\ \vdots & \vdots & \ddots & \vdots \\ S_{iN} & S_{KN} & \cdots & S_{NN} \end{vmatrix} V \begin{vmatrix} \bar{\epsilon}_l\bar{\phi}_j & \bar{\epsilon}_l\bar{\phi}_K & \cdots & \bar{\epsilon}_l\bar{\phi}_N \\ S_{jK} & S_{KK} & \cdots & S_{NK} \\ \vdots & \vdots & \ddots & \vdots \\ S_{jN} & S_{KN} & \cdots & S_{NN} \end{vmatrix} , \tag{4}$$

where phase factors ± 1 have been ignored because they are eliminated by the square taken later anyway, and $S_{ik} = \langle \phi'_i \,|\, \phi_K \rangle$, etc., ... Expanding the first determinant into its co-factors we obtain

$$\phi_c\phi_i\,|\,i\,| + \phi_c \sum_{n=K}^{N} (-1)^{K+n+1}\phi_n\,|\,n\,|\ , \tag{5}$$

where the nth co-factor is defined,

$$|\,n\,| = \begin{vmatrix} S_{iK} & S_{KK} & \cdots & (K\neq n) & \cdots & S_{NK} \\ \vdots & \vdots & & & & \vdots \\ S_{iN} & S_{KN} & \cdots & (K\neq n) & \cdots & S_{NN} \end{vmatrix} . \tag{6}$$

Following Davis and Feldkamp,[15] we can also take advantage of a basic property of determinants that any multiple of a column or row can be subtracted from any other column or row, reducing the first determinant to

$$\phi_c\tilde{\phi}_i\,|\,i\,| + \phi_c \sum_{n=K}^{N} (-1)^{K+n+1}\tilde{\phi}_n\,|\,n\,|\ , \tag{7}$$

where

$$\tilde{\phi}_i = \phi_i - \sum_{m=K}^{N} S_{im}\phi'_m\ . \tag{8}$$

Utilization of the first term only in Eqs. (5) and (7) and correspondingly in the expansion of the second determinant in Eq. (4) leads to the FS and OFS rules, respectively,

$$W(\epsilon) = \frac{2\pi}{\hbar}\,|\,\langle \phi_c\bar{\epsilon}_l \,|\, V \,|\, \phi_i\bar{\phi}_j \rangle\,|^2\,|\,i\,|^2\,|\,j\,|^2\ , \tag{9}$$

$$W(\epsilon) = \frac{2\pi}{\hbar}\,|\,\langle \phi_c\bar{\epsilon}_l \,|\, V \,|\, \tilde{\phi}_i\tilde{\bar{\phi}}_j \rangle\,|^2\,|\,i\,|^2\,|\,j\,|^2\ , \tag{10}$$

for the Auger process. The determinants $|\,i\,|$ and $|\,j\,|$ include the imperfect overlap (i.e., generally less than unity); these factors reduce the principal Auger intensity in a manner known as the Anderson orthogonality catastrophe[26] in metals.

B. Validity of the FS and OFS rules

Examination of the higher-order terms in Eqs. (5) and (7) establishes the validity of the FS and OFS rules. To determine their magnitude relative to the first terms, we simplify by assuming that the co-factors $|\,n\,|$ $(n\neq i)$ are approximately equal. As illustrated by results of a small cluster calculation in Fig. 1, the S_{ij} behave very much like $\langle H \rangle/(E_i - E_j)$ as one would expect from a normal perturbation-theory expansion. Assuming ϕ_i is sufficiently below the Fermi level, we have $S_{iK}, S_{iK+1},\ldots,S_{iN} \ll 1$, indicating $|\,n\,|$ is $O(S_{ik})$ (i.e., of the order S_{ik}). We can also expand ϕ_i

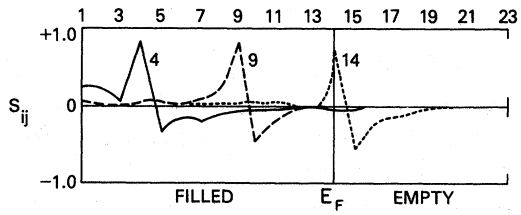

FIG. 1. A plot of the overlap or projection coefficients S_{ij} as defined in Eq. (11) illustrating the $\langle H \rangle/(E_i - E_j)$ behavior of the coefficients. These are typical results of solving a parametrized Hamiltonian for a 125-C-atom cluster in a honeycomb lattice appropriate for graphite (Ref. 46). The plot shows the final-state eigenfunctions 4, 9, and 14 projected onto the initial-state eigenfunctions 1–23 (i.e., the p_π eigenfunction having a_1 symmetry).

within our single-band model,

$$\phi_i = \sum_{n=1}^{N} S_{in}\phi'_n \ . \tag{11}$$

Inserting these approximations into Eqs. (5) and (7) gives

$$\phi_c\phi_i \,|\, i \,| + \phi_c \left[\sum_{m=1}^{N} \phi'_m A_m \right] O(S_{iK}) \ , \tag{5'}$$

$$\phi_c\tilde{\phi}_i \,|\, i \,| + \phi_c \left[\sum_{m=1}^{K-1} \phi'_m A_m \right] O(S_{iK}) \ , \tag{7'}$$

where

$$A_m = \sum_{n=K}^{N} (-1)^{K+N+1} S_{mn} \ .$$

Obviously

$$A_m \approx S_{mK} \quad \text{for } m < K \ ,$$

and

$$A_m \approx S_{mm} \approx 1 \quad \text{for } m \geq K \ .$$

The different limits on the summations in Eqs. (5') and (7') now critically enter. The sum from $m=1$ to $K-1$ is of the order of a weighted average of $S_{mK}(S_{\bar{m}K})$ times the initial local charge ρ'_{occ}; the sum from K to N is of the order of the integrated initial unoccupied LDOS (ρ'_{unocc}). Thus Eqs. (5') and (7') can be written

$$\phi_c\phi_i \,|\, i \,| + O(\rho'_{\text{occ}} S_{\bar{m}K} + \rho'_{\text{unocc}}) O(S_{ik}) \ , \tag{12}$$

$$\phi_c\tilde{\phi}_i \,|\, i \,| + O(\rho'_{\text{occ}} S_{\bar{m}K}) O(S_{ik}) \ , \tag{13}$$

where in general $\rho'_{\text{occ}} S_{\bar{m}K} < \rho'_{\text{unocc}}$.

Equations (12) and (13) reveal some interesting characteristics about the validity of the FS and OFS rules. Both rules approach the exact evaluation of Eq. (4) as $S_{iK} \simeq \langle H \rangle / (E_i - E_K)$ goes to zero, i.e., for energies significantly below the Fermi level. The error in the OFS rule is significantly smaller than in the FS rule, by the additional factor

$$S_{\bar{m}K} / (S_{\bar{m}K} + \rho'_{\text{unocc}} / \rho'_{\text{occ}}) \ ,$$

explaining its increased accuracy near the edge. Obviously for the case of no screening, the FS and OFS results approach the exact result. However, Eqs. (12) and (13) also indicate this is true for "complete" screening; i.e., when a localized state of measure $\simeq 1$ drops out of the band. In this instance $S_{\bar{m}K} \approx S_{1K} \ll 1$ and $\rho'_{\text{unocc}} \ll 1$ ($m=1$ is the localized state).

The FS and OFS results equal the exact when the band is fully occupied in the initial state [$A_m = 0$ in Eqs. (5') and (7')], but this is only true in our single-band model. In a multiband model Eq. (11) becomes

$$\phi_i = \sum_{n=1}^{N} S_{in}\phi'_n + \sum_{m=1}^{\infty} S_{im} f'_m \ , \tag{14}$$

where the first summation involving orbitals of the same band accounts for electron transfer, the second summation accounts for atomic relaxation.[27] For Eq. (14) to be rigorously valid, the second summation must include all other states, even the "Rydberg-type" and continuum orbitals ϵ_l. Since bands of these higher Rydberg-type and continuum orbitals are most certainly unoccupied, they should also be included in the determinants of Eq. (5), hence

$$\tilde{\phi}_i = \phi_i - \sum_{n=K}^{N} S_{in}\phi'_n - \sum_{m=1}^{\infty} S_{im} f'_{im} = \sum_{n=1}^{K-1} S_{in}\phi'_n \ . \tag{15}$$

We see that in this case $\tilde{\phi}_i$ and ϕ_i are not equal even for a filled conduction band, and thus the FS and OFS rules are not generally the same for the filled band. This arises because the atomic relaxation, not allowed for in the single-band model, remains to be projected out of ϕ_i.

Equation (15) reveals an interesting point concerning the Auger intensity. Away from the Fermi level the intraband projection is small. However, the interband projection is relatively energy invariant, it makes a contribution across the entire band. This indicates the orthogonalized final state can be represented by local charge populations similar to the final state; however, the atomic orbitals are more similar to the relaxed initial state; i.e., the line shape is given by the final local density of states (LDOS) as indicated previously, the Auger area is given by an initial-state atomic Auger matrix element times the total local charge in the initial state. The latter point is consistent with the basic sum rules of Grebennikov *et al.*[14] as indicated above for x-ray emission.

Two points of practical importance can be made here. In our previous theoretical work on several systems,[2,28–30] we utilized semiempirical atomic Auger matrix elements. This obviously includes the atomic relaxation effect. Here we normalize the Auger intensity of the FS and OFS rules to that given by the initial state. In doing this we ignore what we call final-state shakeoff (see Sec. II B) and eliminate the need for evaluation of $|\, i \,|^2$ and $|\, j \,|^2$ in Eqs. (9) and (10). Thus we have scaled out the Anderson orthogonality factors. In free-electron metals Schulman and Dow[31] have shown that the Anderson orthogonality factors

which decrease the intensity are approximately canceled by the "replacement" transitions which increase the intensity (i.e., these are competing many-body effects). The normalization to the initial-state intensity causes the FS and OFS results to again equal the exact when the band is fully occupied in the initial state.

Not only is the total intensity determined by the initial state, but to within the validity of the one-electron band model (e.g., negligible configuration mixing), the individual local angular-momentum Auger contributions ll' (e.g., $ll'=ss$, sp, or pp) are determined by the initial state. The intensity of the ll' contributions are individually determined by the initial state if they mix separately into different symmetry orbitals. This follows because orbitals of different symmetry (e.g., orbitals belonging to different irreducible representations of the point group) are orthogonal regardless of whether they are evaluated in or out of the presence of a core hole, and consequently the final-state orbitals of a particular symmetry project onto initial-state orbitals only of the same symmetry. This is a feature of particular interest to the Auger process. Although also true in x-ray emission and absorption, the $\Delta l=\pm 1$ selection rule dictates that normally only $s\,(p)$ density of states (DOS) are observed in a single $L_{23}(K)$ spectrum. In the Auger process, separate ss, sp, and pp contributions are often observed.

Finally, one further point concerning Eq. (15). Davis and Feldkamp[15] labeled Eq. (8) for x-ray emission the OFS rule. This seemed appropriate as the final-state holes are *orthogonalized* to the initial-state holes. However Eq. (15) which is more general implies that the terminology might better be the "projected final-state (PFS) rule" since the final state is *projected* onto the occupied electron orbitals. We will, however, continue to use OFS rather than increase the already large number of three letter acronyms in the literature.

C. Electron shakeoff and the final-state rules

In our earlier work,[2,28] we determined a shake-Auger line shape and added it to the normal Auger line shape to obtain the total. The shake contribution arises from a relaxation of the system around the initial core hole. How do these shake contributions enter in the context of the final-state rules? To understand this, we first consider the ionization process creating the core hole. We could do this in the context of configuration interaction (CI) theory as presented by Martin and Shirley[32]; however, for our purpose here we simplify the notation and consider only the yield of the various processes. In the sudden approximation the total ionization yield, $W^I_{\rm tot}$ has the contributions,

$$W^I_{\rm tot}=W^I_O+\sum_{n=\rm SU}W^I_n+\sum_{m=\rm SO}W^I_m\ , \tag{16}$$

where we have separated the shakeup and shakeoff (SU and SO) contributions. As indicated earlier[27] shakeup arises from electron transfer configurations in the CI expansion, shakeoff primarily from configurations allowing for atomic relaxation. The "initial-state" shakeoff causes an Auger satellite contribution shifted down in electron energy; we determine its line shape separately. The initial-state shakeup generally causes a smaller Auger satellite intensity shifted either down or up in electron energy; we include it in the parent Auger line shape[28] (i.e., $W^I_P=W^I_O+\sum_{n=\rm SU}W^I_n$).

The Auger process which follows, again leaves the system with no core hole causing the orbitals to relax back to what they were in the ground state (if we ignore screening due to valence-state holes). Thus the total Auger yield at energy E, $W^A_{\rm tot}(E)$, is given by the contributions:

$$W^A_{\rm tot}(E)=W^I_P\left[W^A_{PO}(E)+\sum_{n=\rm SU}W^A_{Pn}(E)+\sum_{m=\rm SO}W^A_{Pm}(E)\right]. \tag{17}$$

The last terms include final-state shakeup and shakeoff contributions. As indicated, shakeoff generally dominates shakeup. Whereas initial state shakeoff produces Auger satellites significantly shifted in intensity from the parent peaks, final-state shakeoff introduces, several eV down from the parent peak, extremely broad features which are often indistinguishable from the background. This is at least true for atoms and small gas phase molecules[33–35] which are the only cases for which final-state shake has been considered. Provided the shakeoff process reduces the parent contributions uniformly across the band, which seems reasonable, we can ignore final-state shake and normalize the intensity to that given by the initial state, i.e.,

$$\int\left[W^A_{PO}(E)+\sum_{n=\rm SU}W^A_{Pn}(E)+\sum_{m=\rm SO}W^A_{pm}(E)\right]dE=1\ .$$

Thus we can write

$$W^A_{\rm tot}(E)=\left[\frac{W^I_P}{\int W^A_{PO}(E)dE}\right]W^A_{PO}(E)\ . \qquad (18)$$

Within the FS rule, normalization is performed for each ll' contribution; $W^A_{PO}(E)$ is given by a two-electron atomic Auger matrix element times an appropriate fold of the final DOS. The shake-Auger yield $W^{S\text{-}A}_{\rm tot}(E)$ can be given by the expression

$$W^{S\text{-}A}_{\rm tot}(E)=\sum_{m=\rm SO}\left[\frac{W^I_m}{W^I_p}\left[\frac{N-i}{N}\right]_m W^A_{\rm tot}(E')\times\delta(E-E'-\Delta E_m)\right], \qquad (19)$$

where the factor $[(N-i)/N]_m$ is a statistical weight to account for the additional valence shake hole and ΔE_m is the satellite shift, both defined previously.[28,29]

III. DISCUSSION

We test the validity of the FS rule for several systems by comparison with experiment. The molecular systems, with the atomic s and p orbitals split by a large covalent interaction into bonding and antibonding orbitals, provide an excellent test of the appropriateness of the initial or final local MO populations. The relative local populations may be significantly altered in the bonding and antibonding orbitals upon introduction of a core hole because of the reverse flow of charge in these orbitals. We consider only molecules where the final-state valence holes are delocalized about the entire molecule or oxyanion (e.g., NO_3^-).[2] For such molecules, we believe that valence-hole screening effects are small, and consequently we can approximate the Auger final DOS with results of theoretical calculations on the ground state. Through out the remainder of this paper we use the words "final state" and "ground state" synonymously to describe Auger intensities or local populations.

Table I contains a summary of results for three molecularlike systems, systems where large configuration mixing effects do not occur. The O *KVV* Auger line shape for O_2 (Fig. 2) shows three clearly resolved features. Their origin has been determined by Dunlap *et al.*[30] who performed LCAO-$X\alpha$ calculations for O_2 (with or without a core hole) and quantitatively interpreted the O_2 line shape. Auger intensities, determined by utilizing the initial- and final-state $X\alpha$ populations, are compared with the relative experimental intensities in Table I. Screening effects in the e_g and e_u orbi-

TABLE I. Comparison of actual Auger intensities with those obtained from initial- and final-state populations.

O_2 O *KVV* (Ref. 30)	$\pi_u^{-1}2\sigma_u^{-1}$	$\pi_u^{-1}(\pi_u,3\sigma_g)^{-1}$	$\pi_g^{-1}(\pi_u,3\sigma_g)^{-1}$
$X\alpha$ initial state	2.0	6	1.6
$X\alpha$ final state	1.9	6	2.8
Expt.	2.3	6	4
C_2H_6 C *KVV* (Ref. 36)	$1e_u^{-2}$	$1e_u^{-1}1e_g^{-1}$	$1e_g^{-2}$
RHF-SCF initial state	68	16	1
RHF-SCF final state	0.9	1.9	1
Full theoretical matrix element	1.2	3.0	1
NO_3^- N *KVV* (Ref. 28)	$2e'^{-2}$	$2e'^{-1}(4e',3e',1a_2'')^{-1}$	$(4e',3e',1a_2'')^{-1}$
$X\alpha$ initial state	1	7.4	13
$X\alpha$ final state	1	5	2.5
Empirical fit to data	~1	~5	~2.5

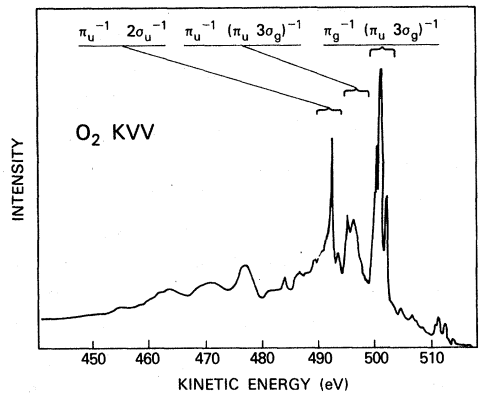

FIG. 2. Experimental O_2 *KVV* Auger spectrum as reported by Siegbahn *et al.* (Ref. 48). The source of the three major features has been indicated as determined by Dunlap *et al.* (Ref. 30).

tals of ethane are even more pronounced. Hartree-Fock self-consistent-field calculations have been performed by Jennison[36] again with or without a core hole. The C *KVV* Auger contributions arising from the e_u^{-2}, e_u^{-1}, e_g^{-1}, and e_g^{-2} hole configurations are not resolved experimentally; however, comparison of the initial- and final-state Auger intensities can be compared with results from a full evaluation of Eq. (4) as reported by Jennison. Finally the NO_3^- anion in the highly ionic $LiNO_3$ crystalline lattice may be treated as a separate molecular ion.[28] Auger intensities obtained from initial- and final-state $X\alpha$ populations are compared with a set of "empirical" populations in Table I. The $X\alpha$ populations are also used to generate a theoretical Auger line shape and compared with the experimental line shape in Fig. 3. The empirical populations are those populations which are optimally consistent with O and N $K\alpha$ x-ray emission data, photoemission data, and the N *KVV* Auger line shape.[28] In all three systems, Auger intensities determined from the final-state population give satisfactory agreement with the experimental data (or the full theoretical result); those from the initial-state populations give poorer agreement. These results support the basic feature of the FS rule; i.e., that the Auger line shape can be adequately interpreted from the final LDOS.

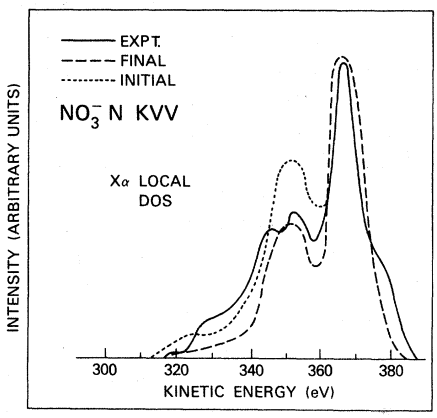

FIG. 3. Comparison of the experimental N *KVV* Auger line shape from $LiNO_3$ (solid) with that calculated utilizing the $X\alpha$ LDOS from the initial- (dotted) and the final- (dashed) state wave functions. Details of the methods involved in determining the Auger and shake-Auger line shape are given in Ref. 28.

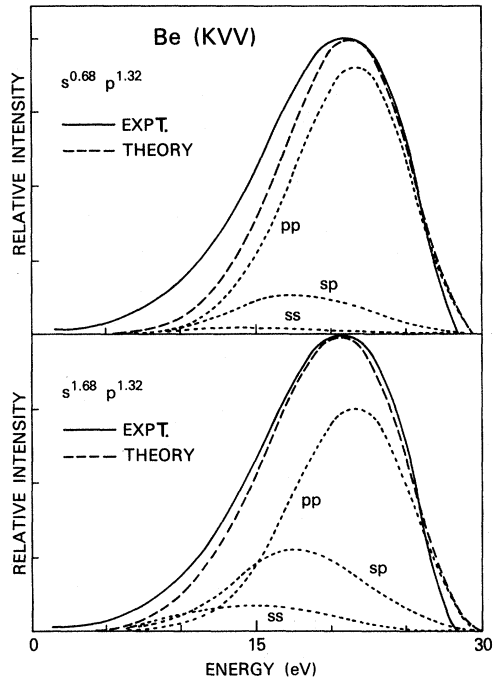

FIG. 4. (Top) Comparison of the experimental Be *KVV* Auger line shape with that calculated utilizing a HF-SCF local DOS from the final state (Ref. 5). (Bottom) Same as the top except the relative *ss*, *sp*, and *pp* areas are determined by the initial state. Complete *s* electron screening is assumed in the initial state.

Examination of Auger data from metals provides a better test of the second feature of the FS rule; i.e., that the relative *ll'* Auger intensities are determined by the initial state. Because of the smaller covalent interaction in metals, each Auger angular momentum contribution normally introduces a single Auger feature. In some metals these are sufficiently resolved to determine their individual areas. We again assume that the final-state valence holes are delocalized about the solid. This will be true when the hole-hole repulsion is less

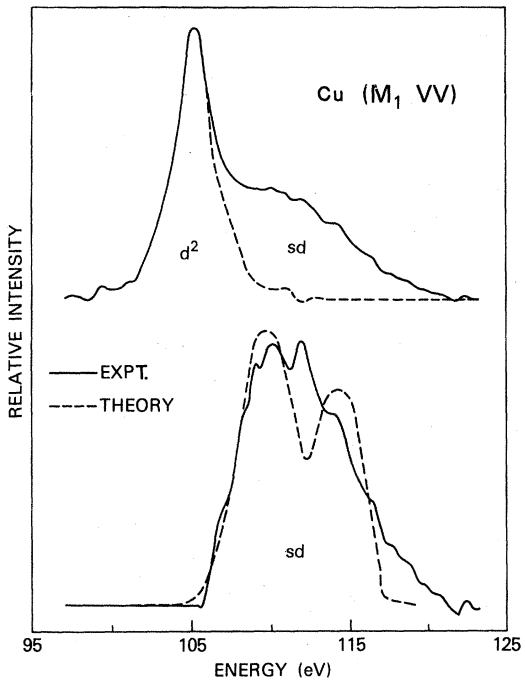

FIG. 5. (Top) The Cu M_1VV experimental Auger spectrum (solid line) as reported in Ref. 6. The narrow localized d^2 contribution is indicated by the dotted line, the difference represents the bandlike *sd* contribution. (Bottom) Comparison of the *sd* Auger contribution as obtained above (solid) with the calculated Auger line shape (dotted). The calculated line shape is obtained from a final LDOS but with the relative *sd*/*dd* area increased by a factor of 2 consistent with the $d^{10}s^2$ initial-state configuration, if one assumes complete *s* electron screening (Ref. 6).

than the valence bandwidth as indicated by the Cini-Sawatzky[37] theory. In this instance, the ground LDOS is indeed an excellent approximation to the Auger final LDOS.

The calculated Be *KVV* Auger line shape as determined from the final LDOS, and with the relative areas determined from the final- and initial-state electron configurations, is compared with experiment in Fig. 4.[5] It was assumed by Jennison[5] when making these calculations that the screening charge is purely *s* like in Be. Recent data on Si, Mg, Al, and Na (Ref. 4) also indicates the screening charge is purely *s* like. Thus screening increases the *ss* and *sp* Auger contributions relative to the *pp* and improves the agreement with experiment.

The Cu M_1VV line shape contains a narrow localized *dd* contribution at lower energy, and a *sd* contribution which reflects a fold of the *s* and *d* final LDOS.[6] The calculated fold of the *s* and *d* LDOS agrees reasonably well with the experimental as shown in Fig. 5, provided its intensity is increased by a factor of 2. Thus the ratio of the areas, *sd*/*dd*, clearly reflects the initial electron configuration $d^{10}s^2$, rather than the final, $d^{10}s$. This again assumes *s* screening in the initial state.

From the work on Be and Cu,[5,6] Jennison *et al.* first noted the success of utilizing a ground state DOS to determine the individual line shapes and altering the relative *ss*, *sp*, and *pp* areas to reflect the initial state. They justified this success by indicating that the initial and ground state DOS must be reasonably similar (aside from a multiplicative constant on the *s* DOS) and thus concluded the Auger line shape reflects the initial state. From an examination of these Cu, Be, and Li *CVV* Auger line shape interpretations,[5,6,38] and the CCV Auger line shapes of Si, Mg, and Al,[4] and some of the $L_{23}M_{45}M_{45}$ line shapes of the transition metals, Kleiman[39] recently concluded that "Auger valence-band spectra appear to measure the atomiclike DOS for a self-consistently screened ion." We must disagree with these conclusions. The initial and final DOS may be very different, indeed they often are. Yet as a result of the FS rule, the individual Auger *ll'* line shapes reflect the final DOS, only the relative *ll'* areas reflect the initial DOS. The final state may, in fact, have a core hole such as for the *CCV* line shapes, in which case the Auger line shape reflects a screened ion, but the *CVV ll'* line shapes will reflect a DOS closer to the ground state, provided valence hole screening does not appreciably alter the DOS. An atomic or localized Auger line shape (when correlation effects dominate) does not reflect the bandlike DOS of either the initial or the final state. The Auger energy, however, indicates the final-state localized valence holes are screened (e.g., the valence *s* electrons screen the localized 3*d* holes in the Cu $L_{23}M_{45}M_{45}$ Auger final state.[6,39] This is consistent with the FS rule.

The Si $L_{23}VV$ Auger line shape[38] is also of interest in this regard. Jennison *et al.* have indicated that screening in Si should have little effect on the Auger line shape.[5] This statement is based primarily on their success in interpreting the $L_{23}VV$ line shape utilizing an unscreened final LDOS with the relative *ss*, *sp*, and *pp* areas also determined by the final LDOS.[38] They argued that the comparatively long-ranged nature of the screening and the need to preserve the Si sp^3 bonding would limit the effect of the core hole. However, Lasser and Fuggle[4] recently showed a large *s* screening contribution in the *CCV* Auger line shapes of Si. This *s*

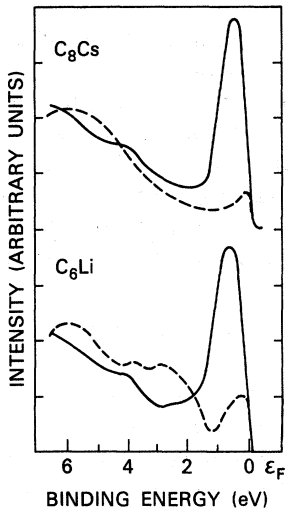

FIG. 6. Comparison of the LDOS as determined in Ref. 43 from a quantitative interpretation of the C *KVV* Auger line shape (solid) with UPS data (dotted) for the intercalated graphite systems C_8C_s and C_6Li.

screening should significantly increase the *ss* and *sp* Auger intensities contributing at the lower energies in the $L_{23}VV$ line shape, but the theoretical line shape, without including screening, already overestimates this intensity.[38] This may be an indication that the FS rule is not obeyed for Si, perhaps because one of our basic assumptions are invalid for this case (e.g., final-state shakeoff may not be negligible). In spite of the already long history of work on the Si $L_{23}VV$ Auger line shape,[38,40–42] it is obvious further work is needed here.

Finally consider the *C KVV* Auger line shape in the intercalated graphite systems, C_6Li and C_8C_s. These Auger line shapes have been examined quantitatively by Murday *et al.*[43] who noted the very large intercalant induced peak near the Fermi level. Figure 6 compares the DOS as obtained from ultraviolet photoemission spectroscopy (UPS) data with that obtained from the Auger line shape. (The DOS in this case is nearly a self-deconvolution of the Auger line shape except that *ss*, *sp*, and *pp* matrix elements have been included in their treatment.) They attributed the much larger intercalant peak in the Auger determined DOS to initial-state screening of the core hole.

Several authors have previously reported the existence of a core excitonic state which plays an important role in the screening of the C 1*s* core hole in graphite and intercalated graphite. Mele and Risko[44] observed the electron energy-loss spectrum of stage-1 $FeCl_3$ intercalated graphite and quantitatively related the core exciton spectrum to the initial distribution of empty states in the presence of the core hole. Van Attekum and Wertheim[45] showed that the C 1*s* line shape of graphite in photoemission is determined by an excitonic state near the Fermi edge in the hole DOS, and suggested that the excitonic spectrum is singular at the Fermi edge.

Utilizing a parametrized self-consistent-field (SCF) Hamiltonian with parameters determined from $X\alpha$ calculations on C and C_2, Dunlap *et al.*[46] determined the $P\pi$ DOS for a 109-atom cluster, and utilizing the OFS rule qualitatively accounted for the enhanced Fermi-level peak in C_6Li. Results of this calculation are summarized in Fig. (7); the $P\pi$ DOS are given with and without a core hole for C_6Li. The excitonic level clearly appears just below the Fermi level in the initial state as expected [Fig. 7(a)]. It is of course not singular in this cluster model. The excitonic state within 2 eV of E_F contains ~ 0.23 electrons of the total 0.6 electron $P\pi$ screening charge.

Figure 7(c) shows the OFS transition DOS; the

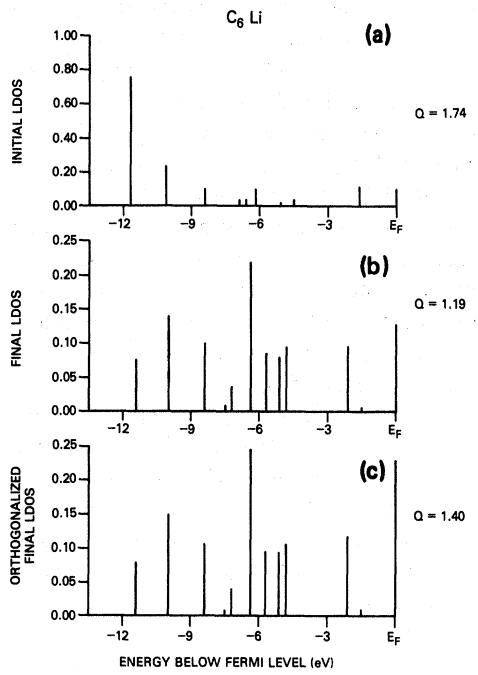

FIG. 7. (a) The P_π DOS local to a core hole as determined for a 125-C-atom cluster in a graphitic lattice utilizing a parametrized Hamiltonian (Ref. 46). (b) The p_π DOS appropriate to the final state (no core hole) determined as above. (c) The OFS rule non-normalized transition DOS obtained from the DOS in a and b above and use of Eq. (10). The normalized OFS rule DOS can be obtained by multiplying each peak by the ratio of the total charges, 1.74:1.40.

self-fold of this would give the P_π^2 Auger contribution. Here the effects of the OFS rule are clearly evident. Ignoring final-state shakeup, the total charge under the normalized OFS excitonic and intercalant induced peak (they both contribute to the Auger peak just below the Fermi level) now contains ~ 0.45 electrons of the total $1.74P\pi$ local charge. This is less than the ~ 0.6 electrons determined from the experimental Auger peak[43] in C_6Li; however, the OFS rule appears to generally underestimate the edge enhancement compared to the exact.[12,13] The approximation of an infinite lattice by a finite cluster will also cause an underestimate of the edge effects. These points have been discussed in more detail in Refs. (43) and (46). It seems clear, however, that electron screening of the core hole in the initial state does play a role in enhancing the Auger intensity just below the Fermi level, and that the OFS rule is adequate for qualitatively examining this effect. It is interesting to note in passing that the OFS transition DOS does faithfully reflect the final DOS for energies >2 eV below E_F.

Although apparently observed in C_6Li, why are the OFS effects (i.e., enhancement near the Fermi level) not more evident in metal Auger line shapes? Whereas edge singularity effects in the L_{23} x-ray emission spectrum of Si, Al, Mg, and Na are clearly evident, they are not seen in the corresponding *KVV* Auger spectra. The explanation for this is basic to the Auger process. In the *sp* band metals, the Auger line shape has *ss*, *sp*, and *pp* contributions; the *pp* generally dominating the spectrum [see Fig. (4)]. Because of the predominant *s* electron screening, only the *ss* and *sp* contributions will exhibit edge effects, but these will appear under the much larger *pp* contribution making them unobservable. The transition metals with unfilled *d* bands experience *d* screening, but very often d^2 Auger holes are localized, drastically altering the d^2 Auger line shapes. In any event, the self-fold of the one-electron DOS to give the Auger transition DOS tends to broaden and reduce the edge effects. Whatever the DOS is, the self-fold is always zero at the edge and starts with a zero or finite derivative.[47] Indeed Natta and Joyces[47] have shown, utilizing the Nozières and De Dominicis asymptotic techniques valid only near the edge, that the most probable case for the Auger process is a zero upper threshold with a *zero* derivative. Apparently the divergent case is a most improbable one for Auger line shapes in metals.

IV. CONCLUSION

The FS rule has been shown to be valid for interpreting Auger line shapes in molecules and solids. It states that the *ll'* Auger line shapes reflect a final DOS, the relative *ll'* areas reflect the initial DOS appropriate for a screened core hole. The OFS rule accounts for the enhanced Auger intensity near the Fermi edge in C_6Li where the screening is *p* like and involves an excitonic state. In metals, edge effects in Auger line shapes appear to be small in most instances; however, screening effects are observed through the relative angular momentum Auger contributions. The FS rule for *CVV* Auger line shapes, and the previously derived FS rule for x-ray emission and UPS indicates that these three spectroscopies all reflect a DOS without a core hole. Thus these spectroscopies complement each other in electronic structure determinations. *CC'V* Auger line shapes reflect, however, consistent with the FS rule, a DOS in the presence of a core hole as confirmed by Lasser and Fuggle.[4] An atomic (localized) Auger line shape does not reflect the bandlike DOS of either the initial or final state.

ACKNOWLEDGMENTS

The author acknowledges valuable discussions with B. I. Dunlap, C. T. White, J. S. Murday, and F. L. Hutson. The author also acknowledges support from the Office of Naval Research.

[1]D. E. Ramaker, Phys. Rev. B 21, 4608 (1980).
[2]B. I. Dunlap, F. L. Hutson, and D. E. Ramaker, J. Vac. Sci. Technol. 18, 556 (1981).
[3]D. E. Ramaker, C. T. White, and J. S. Murday, J. Vac. Sci. Technol. 18, 748 (1981).
[4]R. Lasser and J. C. Fuggle, Phys. Rev. B 22, 2637 (1980).
[5]D. R. Jennison, H. H. Madden, and D. M. Zehner, Phys. Rev. B 21, 430 (1980).
[6]D. R. Jennison, Phys. Rev. B 18, 6996 (1978).
[7]N. D. Lang and A. R. Williams, Phys. Rev. B 20, 1369 (1979); 16, 2408 (1977); A. R. Williams and N. D. Lang, Phys. Rev. Lett. 40, 954 (1978).
[8]K. Schonhammer and O. Gunnarsson, Solid State

Commun. 23, 691 (1977).
[9]G. D. Mahan, Phys. Rev. 163, 612 (1967).
[10]J. W. Gadzuk, J. Electron. Spectrosc. Relat. Phenom. 11, 355 (1977); *Photoemission and the Electronic Properties of Surfaces,* edited by B. Feuerbacker, B. Fitton, and R. F. Willis (Wiley, New York, 1978), p. 111.
[11]G. D. Mahan, Solid State Phys. 29, 75 (1974).
[12]U. Von Barth and G. Grossman, Solid State Commun. 32, 645 (1979); Phys. Scr. 21, 580 (1980); Phys. Rev. B 25, 5150 (1982).
[13]G. D. Mahan, Phys. Rev. B 21, 1421 (1980).
[14]V. I. Grebennikov, Y. A. Babanov, and O. B. Sokolov, Phys. Status Solidi 80, 73 (1977).
[15]L. C. Davis and L. A. Feldkamp, Phys. Rev. B 23, 4269 (1981).
[16]G. Wentzel, Z. Phys. 29, 321 (1928).
[17]D. E. Ramaker and D. M. Schrader, Phys. Rev. A 9, 1980 (1974).
[18]W. H. Miller, Chem. Phys. Lett. 4, 627 (1970).
[19]J. C. Fuggle, M. Campagna, Z. Zolnierek, and R. Lasser, Phys. Rev. Lett. 45, 1597 (1980).
[20]F. J. Himpsel, D. E. Eastman, and E. E. Koch, Phys. Rev. Lett. 44, 214 (1980).
[21]J. C. Fuggle, R. Lasser, O. Gunnarsson, and K. Schonhammer, Phys. Rev. Lett. 44, 1090 (1980).
[22]J. W. Gadzuk and M. Sujic, Phys. Rev. B 12, 524 (1975); J. W. Gadzuk and S. Doniach 77, 427 (1978); J. W. Gadzuk, Surf. Sci. 86, 516 (1979).
[23]M. O. Krause, J. Phys. Chem. Ref. Data 8, 307 (1979).
[24]O. Gunnarsson and K. Schonhammer, Phys. Rev. B 22, 3710 (1980).
[25]M. Ohno and G. Wendin, J. Phys. B 12, 1305 (1979).
[26]P. W. Anderson, Phys. Rev. Lett. 18, 1049 (1967).
[27]W. Domcke, L. S. Cedarbaum, J. Schirmer, and W. von Niessen, Phys. Rev. Lett. 42, 1237 (1979); Chemical Phys. 39, 149 (1979).
[28]F. L. Hutson, D. E. Ramaker, B. I. Dunlap, J. D. Ganjei, and J. S. Murday, J. Chem. Phys. 76, 2181 (1982).
[29]D. E. Ramaker and J. S. Murday, J. Vac. Sci. Technol. 16, 510 (1979).
[30]B. I. Dunlap, P. A. Mills, and D. E. Ramaker, J. Chem. Phys. 75, 300 (1981).
[31]J. N. Schulman and J. D. Dow, Phys. Rev. Lett. 47, 371 (1981).
[32]R. L. Martin and D. A. Shirley, J. Chem. Phys. 64, 3685 (1976); R. L. Martin, B. E. Mills, and D. A. Shirley *ibid.* 64, 3690 (1976).
[33]H. P. Kelly, Phys. Rev. A 11, 556 (1975).
[34]H. Agren and H. Sieghahn, Chem. Phys. Lett. 69, 424 (1980); 72, 498 (1980); H. Agren, S. Svensson, and U. I. Wahlgren, Chem. Phys. Lett. 35, 336 (1975).
[35]K. Faegri, Jr. and H. P. Kelly, Phys. Rev. A 19, 1649 (1979).
[36]D. R. Jennison, Phys. Rev. A 23, 1215 (1981).
[37]M. Cini, Solid State Commun. 20, 605 (1976); Phys. Rev. B 17, 2788 (1978); G. A. Sawatzky, Phys. Rev. Lett. 39, 504 (1977).
[38]D. R. Jennison, Phys. Rev. B 18, 6865 (1978).
[39]G. G. Kleiman, Appl. Surf. Sci. (in press).
[40]P. J. Feibelman, E. J. McGuire, and K. C. Pandey, Phys. Rev. B 15, 2202 (1977); Phys. Rev. Lett. 36, 1154 (1976); P. J. Feibelman and E. J. McGuire, Phys. Rev. B 17, 690 (1978).
[41]D. R. Jennison, Phys. Rev. Lett. 40, 807 (1978).
[42]R. H. Brockman and G. J. Russell, Phys. Rev. B 22, 6302 (1980).
[43]J. S. Murday, B. I. Dunlap, F. L. Hutson II, and P. Oelhafen, Phys. Rev. B 24, 4764 (1981).
[44]E. J. Mele and J. J. Risko, Phys. Rev. Lett. 43, 68 (1979).
[45]P. M. Th. M. Van Attekum and G. K. Wertheim, Phys. Rev. Lett. 43, 1896 (1979).
[46]B. I. Dunlap, D. E. Ramaker, and J. S. Murday, Phys. Rev. B 25, 6439 (1982).
[47]M. Natta and P. Joyes, J. Phys. Chem. Solids 31, 447 (1970).
[48]K. Siegbahn, C. Nordling, G. Johanssen, J. Hedman, P. F. Heden, K. Hamrin, V. Gelius, T. Bergmark, L. O. Werme, R. Mann, and Y. Baer, *ESCA Applied to Free Molecules* (North-Holland, Amsterdam, 1971).